Chemical Engineering Journal 380 (2020) 122533

Contents lists available at ScienceDirect

Chemical Engineering Journal

journal homepage: www.elsevier.com/locate/cej

Regeneration of textile wastewater deteriorated microbial diversity of soil microcosm through bioaugmentation

Swapnil M. Patil[a], Mangesh V. Suryavanshi[b], Vishal V. Chandanshive[c], Mayur B. Kurade[a], Sanjay P. Govindwar[a,*], Byong-Hun Jeon[a,*]

[a] Department of Earth Resources and Environmental Engineering, Hanyang University, Seoul 133-791, South Korea
[b] National Centre for Microbial Resource, National Centre for Cell Science, Pune 411021, India
[c] Department of Biochemistry, Shivaji University, Kolhapur 416004, India

HIGHLIGHTS

- Dye degrading bacteria used for textile dye contaminated soil remediation.
- Augmented soil microcosm showed increase in bioremediation potential.
- Metagenomic analysis reveal textile dye effect on microbial population.
- Functional annotation illustrates role of xenobiotic degradation pathways.
- Augmentation can be used *in-situ* for effective and long-term soil remediation.

GRAPHICAL ABSTRACT

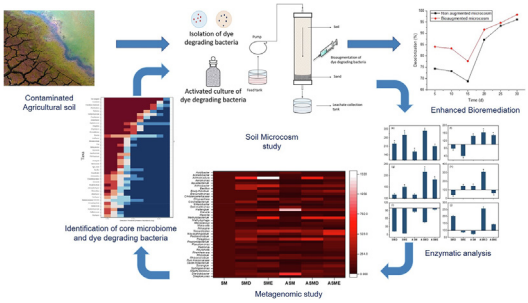

ARTICLE INFO

Keywords:
Microcosm
Metagenomics
Biodegradation
Bioaugmentation
Decolorization

ABSTRACT

Textile dye contamination is a serious concern that reduces soil productivity by destabilizing microbial community structures. Here, we investigated the influence of bioaugmentation on the degradation of a mixture of dyes (MOD) and textile industry effluent (TIE) in soil microcosms using eight different dye-degrading bacteria. The biodegradation potential improved in bioaugmented microcosms, especially in the initial phase. The bioaugmented MOD and TIE microcosms exhibited 98.33% and 94.19% decolorization, and 96.92% and 95% reduction in chemical oxygen demand, respectively, within 30 days. Activities of azoreductase, veratryl alcohol oxidase, lignin peroxidase, and tyrosinase were induced by > three-fold in bioaugmented microcosms. Changes in alpha diversity indicated significant alterations in microbial dynamics due to MOD and TIE feeding. The *Rheinheimera*, *Kocuria*, Ruminococcaceae UCG-010, *Ralstonia* and *Pseudomonas* assemblages were predominant after exposure to MOD and TIE, indicating their key role in dye degradation. The bacteria used for augmentation, namely, *Staphylococcus*, *Bacillus*, *Arthrobacter* and *Pseudomonas* dominantly survived in soil microcosms. Xenobiotic pathways including benzoate, aminobenzoate, chloroalkane and chloroalkene degradation contributed in dye's detoxification as per illustration of functional annotation of metagenomes. This study indicates a mutualistic-symbiotic relationship between augmented bacteria and soil microflora with enhanced detoxification of xenobiotics leading to a sustainable approach for restoration of contaminated lands.

* Corresponding authors.
E-mail addresses: spgovindwar@hanyang.ac.kr (S.P. Govindwar), bhjeon@hanyang.ac.kr (B.-H. Jeon).

https://doi.org/10.1016/j.cej.2019.122533
Received 12 June 2019; Received in revised form 14 August 2019; Accepted 17 August 2019
Available online 19 August 2019
1385-8947/

1. Introduction

Engineered wetlands are environmentally self-sustaining remediation systems that do not require an external energy supply for treatment of contaminated sites. These remediation systems usually involve technologies such as soil amendments, biological permeable reactive barriers, bioremediation, and phytoremediation [1–5]. Cleanup strategies can be used, by combining these technologies to achieve innovative hybrid systems, leading to yet more innovative applications. Contamination of an ecosystem with various xenobiotic pollutants disrupts the microbial community and disturbs the regular functionality of microbiota. The diversity of soil food web communities contributes to the resistance and resilience of ecosystem processes and can guarantee sustainable agrosystem health and productivity [6]. Microbial communities ensure nutrient cycling, functional key steps in biogeochemical cycles (nitrification and denitrification processes) [7,8]. A common threat to soil ecosystems is industrial effluent contamination, especially in agricultural sites located at river banks [9–11]. The textile industry produces an enormous amount of effluent containing recalcitrant dyes, heavy metals, sulfides and detergents [12,13]. Acute or chronic type of toxicity can be resulted from textile dyes exposure [14]. Organisms exposed to high dose of textile dyes and their derivatives adversely affect the normal cellular and defense mechanisms and decrease in microbial diversity and activity was observed in contaminated sites [15]. Moreover, soil fertility and agricultural productivity are also affected by pollution and shifts in bacterial community [16,17].

The soil microbial community is a key constituent of the soil ecology, being responsible for a wide range of biologically significant processes that include maintenance of soil fertility and plant health, with ultimate effect on global carbon cycling and ground water quality [18,19]. Microbe-microbe interactions have a noteworthy impact on the health of the soil microbial community [20] and can synergistically or antagonistically affect other key players, including organisms of higher organisms like plant and protozoa [21]. These interactions can affect the metabolism, growth and diversity of the microbial community [22]. In a stable agricultural ecosystem, the indigenous microbiota also develops supportive relationships with plants that maintains soil productivity [22].

Bioremediation is considered an efficient alternate approach for the removal of textile dyes from a polluted area because it is both environmentally sustainable and cost-effective. The biodegradation of textile dyes has been explored in textile dye contaminated environments using various microorganisms such as *Bacillus* sp. MZS10 [23], *Galactomyces geotrichum* MTCC 1360 [24], and *Penicillium simplicissimum* [25]. Although it has been reported that soil bacteria can degrade textile dyes, *in situ* data on the degradation rates and survivability of bacteria in contaminated soil is still scarce. Information of soil microbial community can be used to illustrate potential risks associated with soil contamination and aid to design possible soil remediation strategies using native resilient bacteria. Along with the role of core microorganisms, data on biodegradation rates and removal efficiencies is essential design and develop sustainable *in situ* bioremediation technologies.

Microcosms offer several advantages such as small size, a controlled condition, short experimental times, better field condition simulation and result can be applied *in situ* in contaminated sites [26]. Here, we present the first detailed investigation results on bioremediation potential of native soil microbiota and the effect of augmenting soil with dye-degrading bacteria on biodegradation rates. The influence of bioaugmentation and exposure to textile dyes on the microbial community structure and changes in their functional dynamics are studied. The survivability of bacteria used for augmentation in the soil microcosms was monitored for a period of 30 d. Xenobiotic degradation pathways were annotated using metagenome data according to KEGG orthology to reveal microbial functions and determine changes in specific functional pathways linked to biodegradation.

2. Materials and methods

2.1. Isolation of potential dye-degrading bacteria from dye-contaminated soil

Dye-degrading bacteria were isolated from dye contaminated soil in a central effluent treatment plant (CETP), Kagal MIDC, Kolhapur, India (GPS location: 16°37′08.8″N, 74°21′12.1″E). The soil sample was added (1% w/v) to nutrient broth containing a mixture of dyes (red HE 3B, green HE 4B, rubin GF1, scarlet GDR, scarlet RR, red HE 8B, ramazol red R, and brilliant blue) at a concentration of 500 ppm and incubated at 37 °C with shaking (120 rpm). After 2 d of incubation, the samples were serially diluted and inoculated on nutrient agar (NA) plates containing a 250 mg L^{-1} dye mixture. Colonies with a clear zone were screened and sub-cultured. The dye degradation potential of these bacteria was tested and bacteria showing a decolorization capacity greater than 75% were selected and stored at 4 °C for further studies (Table S1). Genomic DNA of the screened bacteria was extracted and used for 16S rRNA gene amplification using the primers 27F (5′-AGAGTTTGATCMTGGCTCAG-3′) and 1492R (5′-TACGGYTACCTTGTTACGACTT-3′) [27,28]. The amplified products were purified and sequenced bi-directionally using Big Dye Terminator v3.1 sequencing in an ABI 3500 Genetic Analyzer as per the manufacturer's instructions. The obtained sequences were analyzed using the BLAST (blastn) tool and bacterial identity was determined based on sequences exhibiting > 97% identity.

2.2. Construction of soil microcosms

The soil used for the microcosm study was collected from an agricultural field (top 20–25 cm of the subsurface layer) which had not been previously exposed to textile effluent. The soil was pale brown and fine sandy loam, pH 7.2, and around 56% particles were of diameter of ≤0.01 mm. The collected soil was partially dried and sieved through a 5 mm stainless steel sieve. The sieved homogenized soil (2.5 kg) was placed in a 3-L PVC cylinder 90 cm × 7.6 cm in size (total volume = 4083 mL) with a working volume of approximately 90%. The bottom of the column was filled with a 5-cm layer of sand for efficient percolation (Fig. 1). Six sets of microcosms were prepared for the experiment, as follows: soil (SM), soil with 100 ppm dye mixture (SMD), soil with textile effluent (SME), augmented soil (ASM), augmented soil with 100 ppm dye mixture (ASMD), and augmented soil with textile effluent (ASME). All the microcosms were operated continuously for 30 d.

Dye-degrading bacteria isolated from the soil samples were grown in 30 mL of nutrient broth at 37 °C overnight, with shaking at 120 rpm. All bacterial cultures (5 mL of 5 × 10^8 cells mL^{-1}, each) were mixed and added to the ASM, ASMD, and ASME. The process flow of the daily provision of uncontaminated water or textile effluent is summarized in Table 1. Briefly, the soil-only microcosm (SM) and the augmented soil microcosm (ASM) were supplied with 500 mL of sterile water daily at a flow rate of 1 mL min^{-1} with continuous recirculation. The SMD and ASMD were supplied daily with 500 mL of a mixture of dyes (MOD) (total dye concentration: 100 ppm) at a flow rate of 1 mL min^{-1}. Similarly, the SME and ASME were supplied with 500 mL of textile industry effluent (TIE) daily. Leachates of each microcosm were collected and used for further analysis.

2.3. Characterization of the dye mixture and textile effluent

The MOD, TIE, and the leachates collected at regular intervals from each microcosm were evaluated for color intensity using American Dye Manufacturers Institute (ADMI) color values [29], as well as chemical oxygen demand (COD) and biochemical oxygen demand (BOD) [30]. Total nitrogen content, total phosphorus content, total dissolved solids (TDS), total suspended solids (TSS), and organic carbon content of the

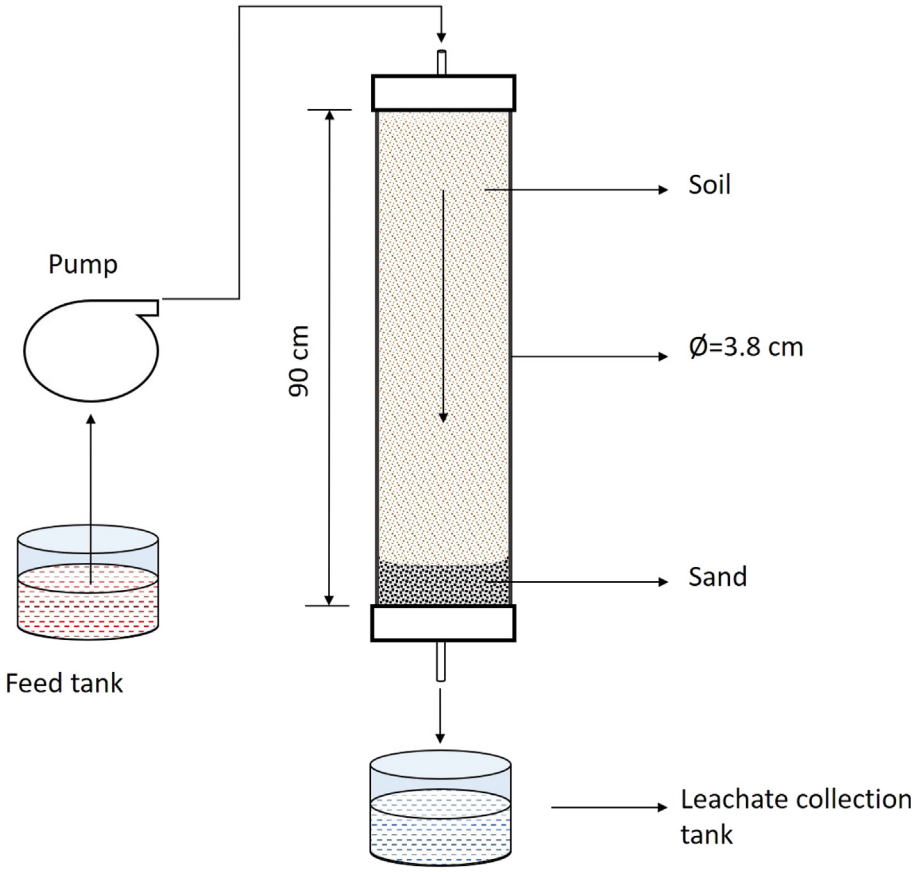

Fig. 1. Schematic representation of the developed microcosm.

textile industry effluent of TIE and leachate were calculated [30]. Heavy metals (cadmium, arsenic, lead, chromium, and mercury) were estimated using an atomic absorption spectrophotometer (Thermofisher AA203) (Table 2) [31].

2.4. Enzymatic analysis of the microcosms

After sieving the soil sample (~2 mm mesh), 5 g were mixed with 40 mL of a sterile 0.9% NaCl solution at 150 rpm for 1 h. A 10 mL soil suspension was transferred to a 15 mL centrifuge tube and homogenized vigorously with glass beads (2 mm in diameter) for 15 min. After suspension was centrifuged at 5000 rpm for 10 min, supernatant was recovered and used further as the enzyme source [32]. The detailed methodology for determination of enzyme activities is provided in the supplementary material.

2.5. Variation of microcosm microbial communities

2.5.1. Sample collection, genomic DNA extraction, and next-generation sequencing

To reveal the influence of exposure to a MOD and TIE and incorporation of species for bioaugmentation, the microbial community structure of each microcosm was studied using 16S rRNA amplicon sequencing analysis. Briefly, the microcosm reactors were disassembled after 30 d and the soil samples from the top, bottom, and middle layers of the soil column were collected, homogenized, and used for total community genomic DNA extraction. DNA was extracted from each microcosm using a soil DNA extraction kit (Qiagen). The extracted genomic DNA was qualified using agarose gel electrophoresis and quantified using a Nanodrop (ThermoFisher Scientific, USA). The V3 region of the 16S rRNA gene was amplified using the universal primers 341F and 518 R [33]. The purified PCR products were end-repaired and ligated with barcode adaptors according to the Ion Xpress™ Plus gDNA Fragment Library Preparation user guide. All ligated amplicons were

Table 1
Experimental conditions and setup of soil microcosms.

No.	Microcosm code	Bioaugmentation	Inlet feed and volume[1]
1	Soil microcosm (SM)	No	Sterile water: 500 mL d^{-1}
2	Soil microcosm with dye mixture (SMD)	No	Mixture of dyes[2]: 500 mL d^{-1}
3	Soil microcosm with industrial effluent (SME)	No	Textile industrial effluent: 500 mL d^{-1}
4	Augmented soil microcosm (SM)	Augmented[3]	Sterile water: 500 mL d^{-1}
5	Augmented soil microcosm with dye mixture (SMD)	Augmented[3]	Mixture of dyes[2]: 500 mL d^{-1}
6	Augmented soil microcosm with industrial effluent (SME)	Augmented[3]	Textile industrial effluent: 500 mL d^{-1}

[1] The feed solution (500 mL d^{-1}) was passed through the microcosms for 30 days.
[2] Mixture of dyes (MOD) (100 ppm): red HE 3B, green HE 4B, rubin GF1, scarlet GDR, scarlet RR, red HE 8B, ramazol red R and brilliant blue.
[3] Overnight grown culture of 8 bacterial strains (5 mL of 5 × 10^8 cells mL^{-1}, each).

Table 2
Characterization of the textile effluent in the augmented and non-augmented soil microcosms.

Parameter	Untreated effluent	Leachate of SME (30 d)	Leachate of ASME (30 d)
ADMI Unit	86 ± 2.9	7 ± 1.57	5 ± 1.06
COD (mg L^{-1})	2800 ± 2.3	476 ± 1.4	355 ± 1.1
BOD (mg L^{-1})	2150 ± 5.2	346 ± 1.12	302 ± 0.86
pH	10.7	9.2	8.0
TDS (mg L^{-1})	9562 ± 9.8	4208 ± 5.17	3541 ± 4.95
TSS (mg L^{-1})	7280 ± 6.3	3310 ± 4.22	2355 ± 4.08
Organic Carbon (%)	1.49 ± 0.48	1.15 ± 0.24	0.98 ± 0.05
Total Nitrogen (mg L^{-1})	7.13 ± 1.9	4.82 ± 1.02	3.17 ± 1.29
Total Phosphorous (mg L^{-1})	10.42 ± 1.4	6.67 ± 1.80	4.96 ± 1.21
Cadmium (mg L^{-1})	0.07 ± 0.003	0.06 ± 0.007	0.06 ± 0.005
Arsenic (mg L^{-1})	2.12 ± 0.02	2.10 ± 0.67	2.05 ± 0.08
Lead (mg L^{-1})	0.42 ± 0.023	0.39 ± 0.016	0.31 ± 0.011
Chromium (mg L^{-1})	1.91 ± 0.05	1.79 ± 0.25	1.52 ± 0.43

Values are the means of three independent experiments (± SEM).

sequenced using an Ion Torrent Personal Genome Machine (Thermo-Fisher Scientific, USA) [34].

2.5.2. Metagenomic data analysis

The obtained raw reads were filtered using the MOTHUR pipeline using the following conditions: length 150 to 200 bp, homopolymer maximum 5, average quality-20 with zero maximum ambiguity to obtain fasta and quality files [35]. All good quality reads were analyzed further using the QIIME (Quantitative Insight into Microbial Ecology) package v 1.9 and the SILVA 123 ribosomal RNA (rRNA) databases was used as the reference dataset at 97% similarity [36]. Core OTUs were estimated as previously described [37]. The Chao1 and Shannon alpha diversity indices were applied using the Mann-Whitney and Kruskal-Wallis statistical tests on rarefied sequence count. Effect of exposed chemicals on microbial abundance at genus level was studied using Principal Component Analysis (PCA) using STAMP. Statistical test was applied using Games-Howell post hoc test variance and Benjamin-Hochberg FDR for correction by removing unclassified reads analyses [38]. The core microbiome at the genus level was computed with 30% sample prevalence and 0.3% relative abundance. The metagenome imputation was done using a previously described method [39]. A closed reference-based OTU picking approach and the latest greengene database 38.8 with a 97% sequence similarity cut-off was used to bin the amplicon sequences. Metagenome prediction was done after normalization of the 16S rRNA gene copy number. Metagenome data was processed to predict KEGG ortholog using obtained OTU table. Venn diagram was prepared in MetaCoMET (Metagenomics Core Microbiome Exploration Tool) and statistical analysis was performed in GraphPad Prism (v6.0) [40].

3. Results and discussion

3.1. Soil microcosm performance with MOD and TIE treatment

The decolorization performance of the MOD- and TIE-treated non-augmented soil microcosms (SMD and SME) increased gradually with time. The decolorization of the MOD in the SMD was 74% on day 5 and further increased to 96% by the end of day 30 (Fig. 2a). The decolorization of the TIE in the SME increased from 68% after 5 d to 92% after 30 d. Similarly, the SMD showed a gradual increase in BOD and COD removal capacity from day 5 until the end of day 30, with values of 76% and 78%, respectively, whereas the SME showed increases of 60% and 84%, respectively, during the same period (Fig. 2b, c). Overall, BOD and COD removal in both microcosms (SMD and SME) was > 95% after 30 d, indicating that the synthetic dyes were efficiently biodegraded in

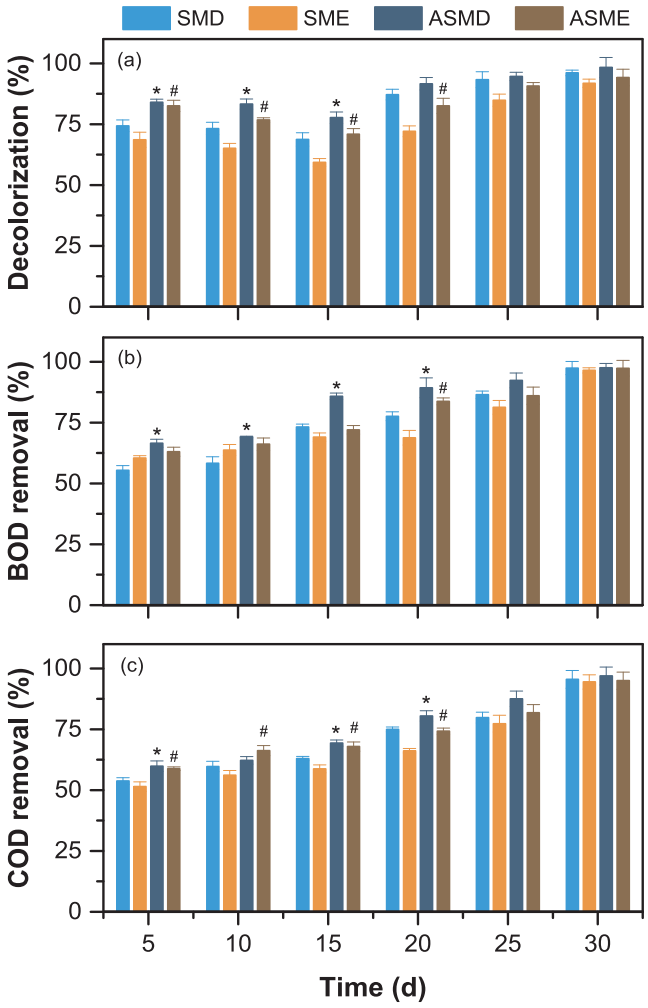

Fig. 2. Reduction in the ADMI value, COD, and BOD of the dye mixture solution and textile industrial effluent in the soil microcosms.

both microcosms by native soil microflora. Unexpectedly, the non-augmented microcosms performed effectively in terms of color and oxygen demand reduction. This suggests that indigenous microflora can degrade xenobiotic organic contaminants under the right conditions. The improved performance of these non-augmented microcosms at later stages (after 15 d) may have resulted from the adaptation of the indigenous microbial community to the toxicant stress [41–44].

Both color and oxygen demand removal capacity were enhanced in the MOD- and TIE-treating bioaugmented soil microcosms (ASMD and ASME). For the ASMD, the decolorization of the MOD in the initial phase (day 5) showed a significant 13% increase, while the BOD and COD removal capacity increased by 20% and 11%, respectively, compared to the non-augmented microcosm (SMD) (Fig. 2). Similarly, the ADMI color values and the BOD and COD removal capacity of the ASME improved by 20%, 4%, and 14%, respectively, compared to the SME, due to the positive effect of bioaugmentation. Bioaugmentation with dye-degrading bacteria in the microcosms decreased the initial lag phase by eliciting high textile dye biodegradation rates. However, significant enhancements in color and oxygen demand removal were observed until day 20, after which the bioaugmented and non-augmented microcosms performed almost similarly. Species with bioaugmentation potential were identified according to 16S rRNA gene sequence analysis and tested for decolorization performance. All these species exhibited > 75% decolorization of a 100 mg L^{-1} dye mixture within 48 h (Table S1); furthermore, the decolorization capabilities of these species using several textile dyes were well documented in earlier studies

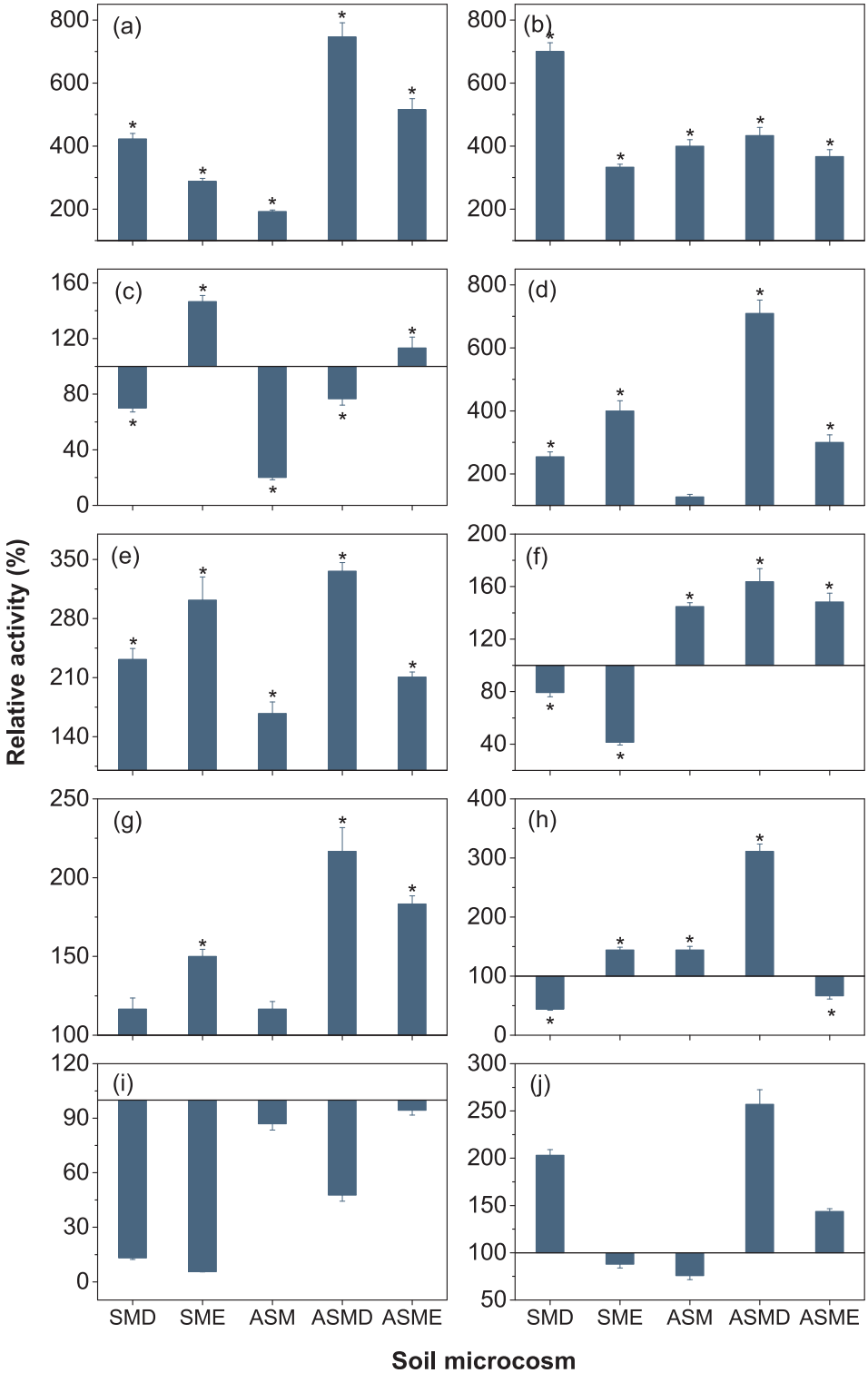

Fig. 3. Enzymatic responses of the different soil microcosms presented as relative induction or inhibition compared to the control soil microcosm (SM); lignin peroxidase (a), veratryl alcohol oxidase (b), laccase (c), tyrosinase (d), azoreductase (e), NADH-DCIP reductase (f), riboflavin reductase (g), peroxidase (h), superoxide dismutase (i), and catalase (j). The enzyme activities of all the soil microcosms were determined at day 30.

[41–44]. Therefore, selection of these species for bioaugmentation of soil microcosms was beneficial for the enhancement of biodegradation of textile dyes. Several additional TIE environmental parameters were also monitored, revealing that the bioaugmented TIE-treated microcosm (ASME) was superior to the non-augmented TIE-treated microcosm (SME) for all effluent quality parameters analyzed, including TDS, TSS, total P, total N, and heavy metals (Table 2). Earlier work on *in situ* remediation of textile dyes in constructed ridges of a high rate transpiration system cultivated with various plants showed a significant decrease in ADMI values [45].

3.2. Enzymatic analysis of soil microcosms

The enzyme activity in the non-augmented soil microcosm (SM) was

considered as the control and was compared to the enzyme activity in the other microcosms (Fig. 3 and Table S2). The SMD and SME showed significant increases in dye-degrading and cell stress-related enzyme activity. The major oxidoreductase enzymes that degrade textile dyes are veratryl alcohol oxidase, laccase, lignin peroxidase, tyrosinase, azoreductase, nicotinamide adenine dinucleotide (NADH)-2,6-dichlorophenol-indophenol (DCIP) reductase, and riboflavin reductase [46]. The activities of veratryl alcohol oxidase (7-fold), lignin peroxidase (4.2-fold), tyrosinase (2.6-fold), azoreductase (2.3-fold), and catalase (2-fold) were significantly induced ($p < 0.05$) in the SMD, whereas the activities of superoxide dismutase, laccase, peroxidase, and NADH-DCIP reductase were inhibited by 0.87-, 0.3-, 0.56-, and 0.21-fold, respectively. For SME, a relatively smaller induction of the activities of major enzymes was observed when compared to SMD. Tyrosinase, veratryl alcohol oxidase, azoreductase, lignin peroxidase, laccase, riboflavin reductase, and peroxidase exhibited up to 4-, 3.3-, 3-, 2.9-, 1.5-, 1.5-, and 1.4-fold induction, respectively ($p < 0.05$), whereas the activities of NADH-DCIP reductase and superoxide dismutase decreased by 0.59- and 0.94-fold, respectively.

The addition of dye-degrading microorganisms to the soil microcosms positively influenced enzyme activity in the ASM, which acted as a bioaugmented microcosm control. Bioaugmentation promoted lignin peroxidase (1.92-fold), veratryl alcohol oxidase (4-fold), azoreductase (1.68-fold), NADH-DCIP reductase (1.45-fold), and peroxidase (1.44-fold) induction ($p < 0.05$) in the ASM. However, laccase, superoxide dismutase, and catalase activities were slightly inhibited by 0.8-, 0.13-, and 0.24-fold compared to the SM. The ASMD showed significant induction ($p < 0.05$) in lignin peroxidase (7.5-fold), veratryl alcohol oxidase (4.3-fold), tyrosinase (7.1-fold), azoreductase (3.4-fold), NADH-DCIP reductase (1.6-fold), riboflavin reductase (2.2-fold), peroxidase (3.1-fold), and catalase (2.6-fold) activities, whereas those of laccase and superoxide dismutase decreased by 0.23- and 0.52-fold, respectively. The ASME exhibited a significant induction ($p < 0.05$) in the activities of lignin peroxidase (5.2-fold), veratryl alcohol oxidase (3.7-fold), tyrosinase (3-fold), azoreductase (2.1-fold), riboflavin reductase (1.8-fold), NADH-DCIP reductase (1.5-fold), catalase (1.4-fold) and laccase (1.1-fold), while peroxidase activity was significantly reduced (0.33-fold). Similar to SME, the ASME presented a relatively smaller induction in the activities of the major enzymes compared to the ASM. The relatively low level of enzyme activity in the SME and ASME may have been due to the inhibitory contaminants in the TIE as they contain numerous geogenic organic contaminants and heavy metals [47].

Overall, augmentation with dye-degrading bacteria in the soil microcosms resulted in a significant induction in dye-degrading enzyme activity that can be correlated with the high levels of decolorization and reduced BOD and COD in both the ASMD and ASME. The cumulative activity of the induced enzymes elicited faster decolorization. Earlier studies have shown the role of enzymes including tyrosinase, lignin peroxidase, laccase, veratryl alcohol oxidase, NADH-DCIP reductase, azoreductase, and riboflavin reductase in the breakdown of dye molecules [48]. Bacterial consortium studies have also shown increased dye decolorization and detoxification by mixed microbial cultures compared to detoxification by individual strains [49,50].

3.3. Analysis of microbial diversity in the soil microcosms

Variations in microbial diversity in the soil microcosms were evaluated using 16S rRNA amplicon sequence. A Venn diagram was used to plot distribution patterns of OTUs suggested that 13.38% of OTUs were shared among the six microcosms (Fig. 4). A change in the microbial profile was observed with exposure to the MOD or TIE. The percentages of unique OTUs for the SM, SMD, SME, ASM, ASMD, and ASME were 12, 13, 20, 20, 17, and 0.31%, respectively. The α-diversity calculated using Chao1 and Shannon indexes indicated the richness and evenness of microbial diversity is drastically affected by MOD and TIE in the microcosms (Fig. S1). The median of both parameters was lowest in the SM and increased in the SMD and SME. Increased richness and diversity were observed in all three augmented microcosms (ASM, ASMD, and ASME) compared to the non-augmented microcosms (SM, SMD, and SME).

The Principal Component Analysis (PCA) indicated that the microcosm treated with similar chemical clustered together, indicating that MOD and TIE have high impact on the microbial communities. The PCA for the microcosms illustrated closer clustering between the SMD and ASMD and between SME and ASME. In contrast, the SM and ASM exhibited some of the larger separations, suggesting that the microbial community from this soil was more sensitive to textile dye and industrial effluent exposure than augmentation (Fig. S2).

3.4. Changes in the microbial communities of soil microcosms and survivability of bacteria used for bioaugmentation

The results of the 16S rRNA amplicon sequencing showed that the Proteobacteria, Firmicutes, Actinobacteria, Acidobacteria, and Chloroflexi were dominant phyla and comprised > 79% of the total soil microbiome in all the microcosms (Fig. 5a). Phyla Proteobacteria was the most profuse phylum in each microcosm, accounting for 49-67% of the total microbial diversity. Species consisting in Proteobacteria are important and abundant in natural environment and essential for fundamental biogeochemical functions. The proteobacteria in soil microcosms consisted of five classes: Alpha-proteobacteria, Beta-proteobacteria, Gamma-proteobacteria, Delta-proteobacteria and Epsilon-proteobacteiria were dominant in dye mixture and industrial effluent microcosms. The dominance of Proteobacteria during textile dye biodegradation was also reported in earlier studies [51]. Other prevalent bacterial phyla identified in all the microcosms were Actinobacteria (9-24%), Firmicutes (2-30%), Acidobacteria (2-4%), Chloroflexi (0.5-6%), and Gemmatimonadetes (0.5-12% of the total microbial abundance). These phyla are commonly found in soil contaminated with pollutants such as oil, dyes, and heavy metals [52–54].

The top 40 dominant generic populations in the studied microcosms are presented in Fig. 5b. The dominant genera in the indigenous soil microcosm (SM) include *Rheinheimera* (15.1%), *Kocuria* (14.9%), Ruminococcaceae UCG-010 (4.83%), *Ralstonia* (3.26%), *Pseudomonas* (3.26%), *Acinetobacter* (2.5%), and *Streptomyces* (1.63%). The *Pseudomonas* and *Streptomyces* are from mycorrhiza helper bacteria group and promote mycorrhiza formation which play a crucial role in N and P cycle in the soil and responsible for transport of C in soil. They accelerate mycelial growth and increase new lateral roots formation [55,56].

Soil exposure to textile dyes significantly influenced the natural microflora of the soil. Some of the significantly inhibited (35%–100%) genera in the textile- and dye-loaded microcosms (SMD, SME, ASMD, and ASME) include *Rheinheimera, Kocuria,* Ruminococcaceae UCG-010*, Micrococcus, Moraxella,* Christensenellaceae R-7 group*, Aeromonas, Enterobacter*, and *Massilia*. Simultaneously, the populations of *Methylobacterium, Bacillus, Pelagibius, Sorangium, Rhizomicrobium, Bradyrhizobium, Nocardioides, Actinomadura, Haliangium, Steroidobacter, Novosphingobium*, and *Arthrobacter* increased significantly ($p < 0.05$), with values ranging from 1.5- to 13-fold. Most of these genera, including *Pseudomonas*, *Bacillus*, *Sphingomonas*, *Aeromonas*, and *Staphylococcus*, are well-known for their biodegradability capabilities [57,58]. Some of the genera that were inhibited in the non-augmented microcosms (SMD and SME) were found to have survived well, and with a large relative abundance, in the bioaugmented microcosms (ASMD and ASME). Experimental analysis demonstrated that all augmented bacteria can not only able to sustain stress of MOD and TIF in soil microbiome, but also increase dye decolorization rate and detoxifying the soil by decreasing COD and BOD. The results indicate that augmented dye degrading bacteria and native soil microbial species have established a potentially mutualistic relationship with xenobiotic degradation pathways. These observations suggest that bacterial

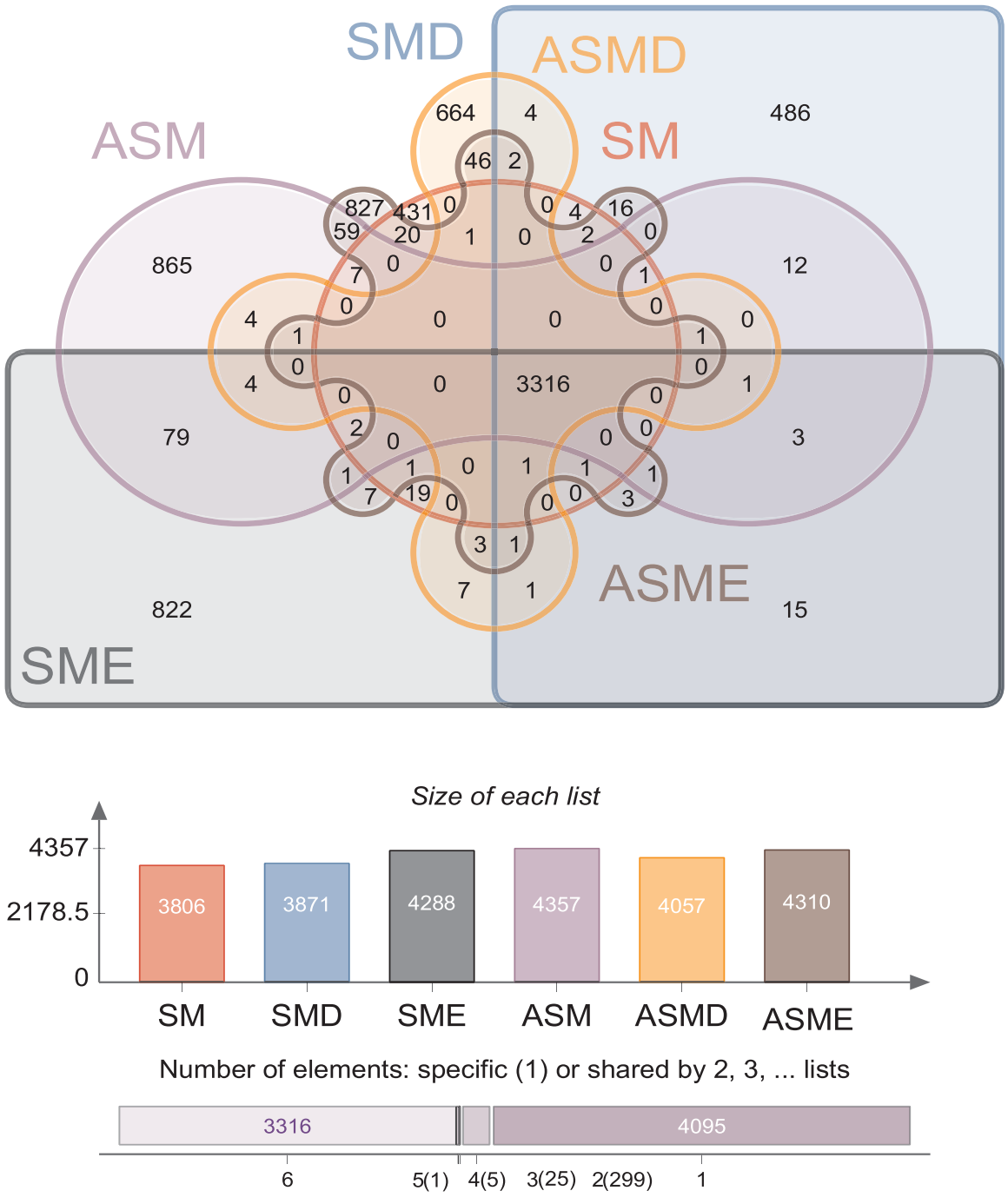

Fig. 4. Venn diagram showing the number of unique and shared operational taxonomic units (OTUs) in the different microcosms. The numbers in the overlapping regions indicate the common OTUs shared between the different groups; the numbers in the non-overlapping regions indicate the number of exclusive OTUs.

bioaugmentation was actively involved in dye biodegradation and minimized dye-induced toxic stress, thus preventing harmful toxic effects on the indigenous microflora.

The 16S rRNA amplicon associated with the dominant phyla were further analyzed at the genus level for a better understanding of the dynamics and abundance of core microbial constituents in all the soil microcosms (Fig. 6). At the genus level, 39 bacterial genera were identified as core microbiota, with 30% sample prevalence and 0.3% relative abundance. The core microbiota was relatively large, even at a 0.3% abundance threshold, and consisted of approximately 65% to 85% of the total bacterial population. As the microcosms were exposed to MOD and TIE, the core genera may have adapted to the textile dyes and are therefore important for dye bioremediation. The bacteria used for bioaugmentation were also an integral part of the core microbiota.

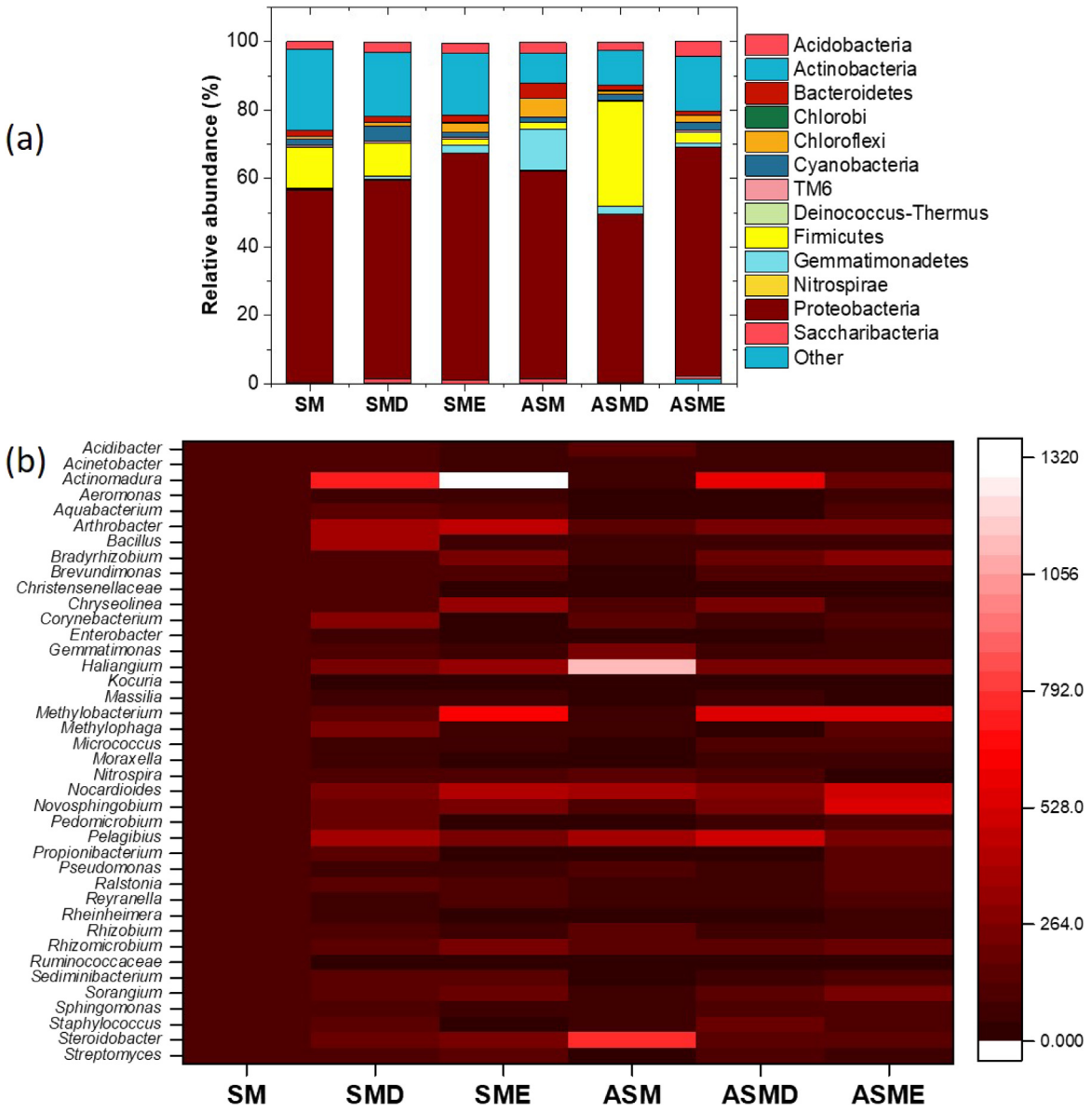

Fig. 5. Phylum-level distribution of Ion Torrent sequences of the different soil microcosms (a); heat map depicting the relative abundance of the dominant microbial taxonomic classes identified in the soil microcosms (b).

Moreover, the genera identified in the core microbiota (other than in bioaugmented soils) have been reported as having the capacity to biodegrade dyes and xenobiotic organic compounds [59].

An earlier study also reported an increase in the soil bacterial population from the rhizospheric area of wetlands cultivated with *Tagetes patula*, *Aster amellus*, *Portulaca grandiflora*, and *Gaillardia grandiflora* contaminated with textile effluent after 30 d, compared to unplanted soil, due to the release of exudates as well as the carbon sources released through dye metabolism [45]. A change in microbial diversity in soil associated with the plants during phytobed augmentation was also reported. The species such as *Bacillus*, *Burkholderia*, *Comomonas*, *Frankia*, *Kocuria*, *Nocardia*, *Pseudomonas* and *Rhodococcus* sp. were shown dye degradation potential with plant synergism [60].

3.5. KEGG pathway analysis

We are interested in metabolic pathways for xenobiotic degradation, because xenobiotics detoxification systems can also degrade textile dyes and its intermediate products. The KEGG orthology analysis indicates presence of abundant enzymes related to xenobiotic pathways in soil bacterial genome. Functional annotation of metagenomes indicates possible contribution of benzoate degradation, aminobenzoate degradation, chloroalkane and chloroalkene degradation, naphthalene degradation etc. pathways may involve in textile dye degradation and detoxification in soil microbiome. Xenobiotic metabolism-associated sequences were identified in the metagenomes are illustrated based on percent relative abundances in Fig. 7. We compared the xenobiotic degradation pathways with reference databases using the SM as a control. The results showed that the SMD, SME, ASM, ASMD, and ASME were enriched with xenobiotic degradation pathways for the catabolism of various xenobiotic compounds, including aminobenzoate, bisphenol, chlorobenzoate, dichlorodiphenyltrichloroethane (DDT), methylnaphthalene, toluene, and xylene (Fig. 8). Interestingly, most of these pathways were significantly enhanced in the ASMD and ASME (bioaugmented microcosms), suggesting that the addition of biodegrading bacteria to these soil microcosms promoted organic pollutant degradation. The overactivation of the xenobiotic degrading pathways illustrate the adaptability of the native microbial species in utilizing the xenobiotic pollutants as sources of energy. These results are in line with the high decolorization capacity of the ASMD and ASME (Fig. 2)

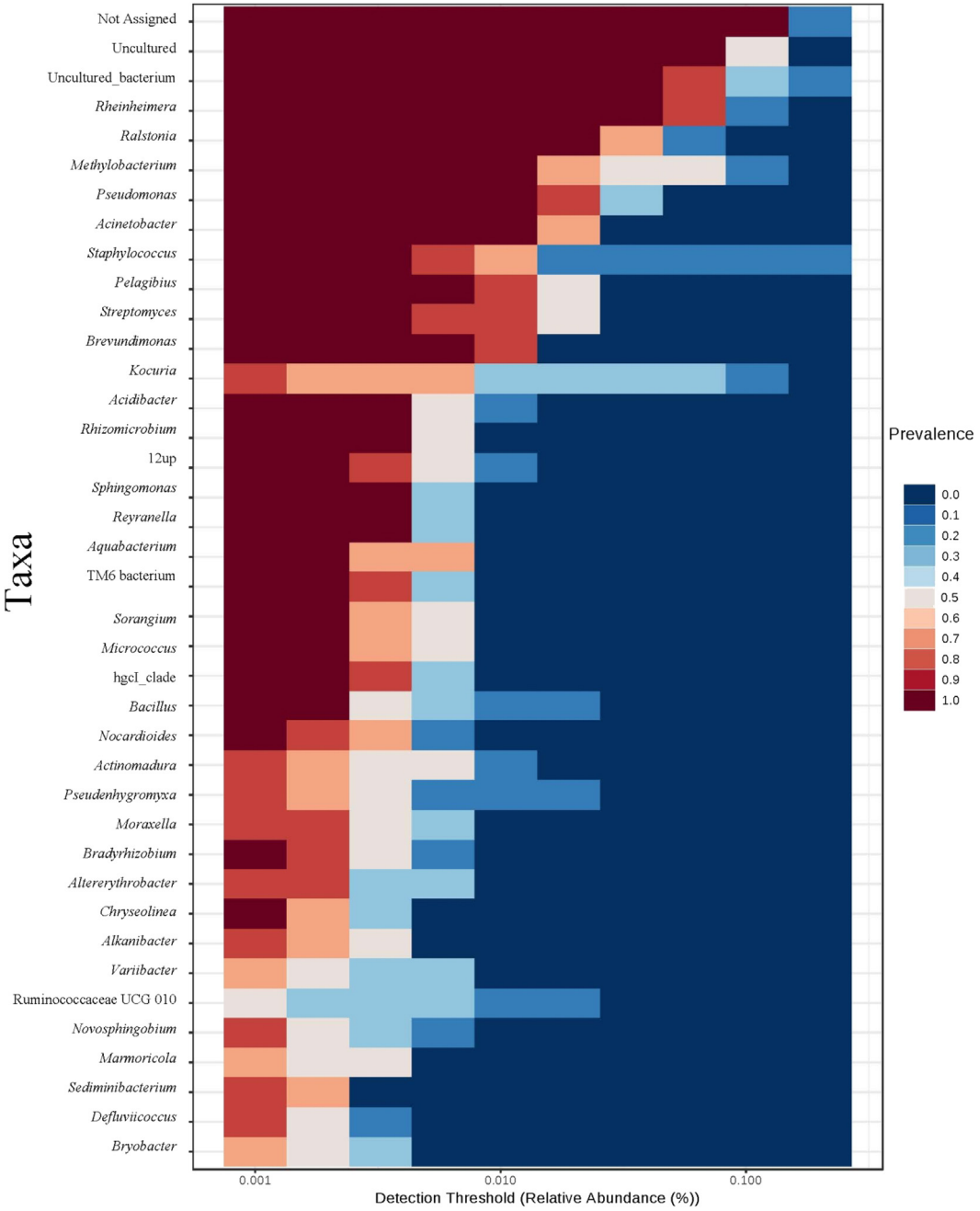

Fig. 6. Heat map of the core-microbiome at the genus level with 30% sample prevalence and 0.3% relative abundance.

observed in this study, as well as the greater induction of dye-degrading enzymes within these microcosms (Fig. 3). Metagenes encoding enzymes involved in the pathway of benzoate degradation were observed in SM (10980), SMD (15923), SME (35524), ASM (33268), ASMD (37906) and ASME (45552) which was most abundant compared to other xenobiotic pathways (Table S3). Anaerobic metabolism of aromatic compounds resulted benzoate as intermediate compound. Phenolic and polycyclic aromatic compounds, toxic to cell, usually degraded into benzoate through a detoxification pathway using enzymes such as lignin azoreductase, peroxidase, laccase, etc. The enzymatic analysis of microcosm supports prediction of functional annotation. The increase in activity of azoreductase, peroxidase and laccase were observed after exposure to MOD and TIE. The intermediate of detoxifying pathway then further degraded through benzoate degradation pathway. Acetyl CoA is the terminal product of benzoate degradation and can be utilized in the citrate cycle. Previous report is also available indicating that *Pseudomonas* species can use benzoate as a carbon and energy source for growth [61]. Thus, for textile dye decolorization and detoxification in the soil, benzoate degradation and its related pathways are very crucial.

Soil and water remediation using biological methods is very promising and cost effective approach. Bioremediation methods are self-sustaining and do not require external power source and any chemical supplements. In this study, no nutrients or media were added to enhance dye degradation. Nutrients required for the growth of microorganisms are fulfilled by soil and effluent. The physical and chemical methods of remediation require controlled conditions, external power and chemical supply, and results in an increase in cost of treatment process [62,63]. Biological treatment of textile effluent is efficiently achieved using bacteria, fungus and plant system. Microbial remediation is comparatively fast method and uses pure and/or mixed microbial cultures along with several types of reactors [1,29,45,60].

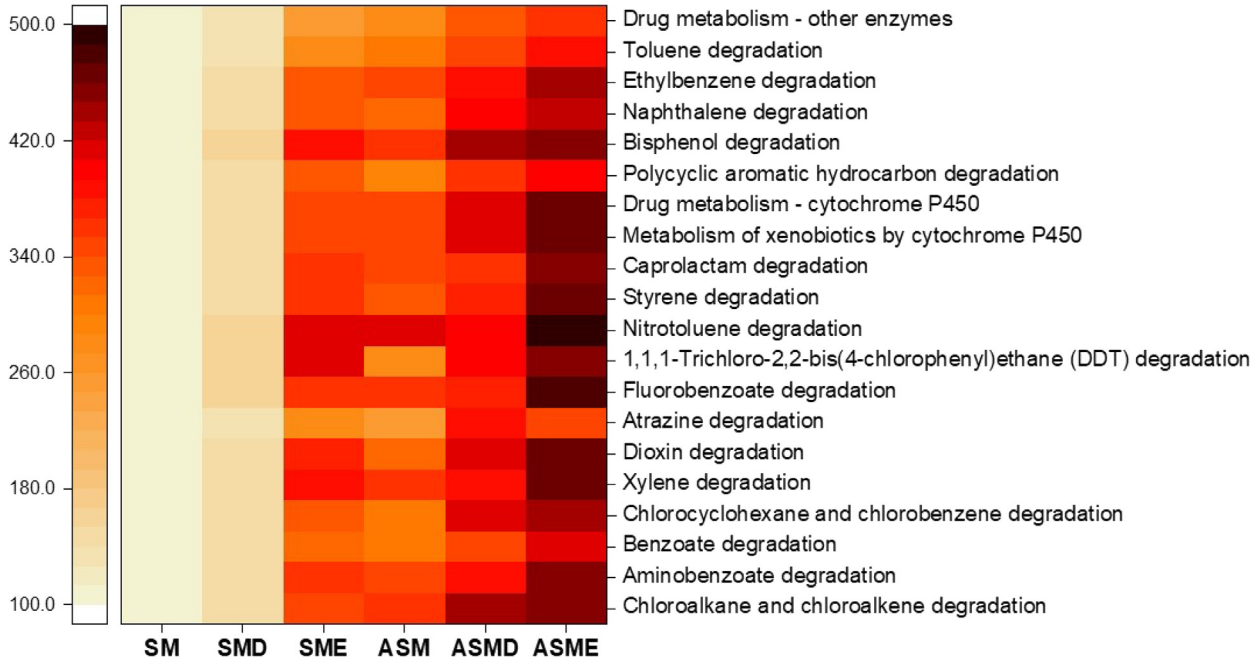

Fig. 7. Relative abundance of xenobiotic metabolism genes identified in the microbial communities of the microcosm expose to dye mixture and textile industrial effluent. Shown is a heat map indicating the relative number of sequence reads associated with KEGG xenobiotic metabolism categories (on the right) identified in each sample (at the bottom). Software used: Statistical Analysis of Metagenomic Profiles (STAMP) software v2.1.3.

Phytoremediation methods are very effective in treatment of textile dyes and effluent, and practically feasible option as it can handle large water volume with minimum management [23,24,43,44,48,50]. Hybrid systems take advantage of both plants, bacterial inoculants and their synergy as observed in floating treatment wetlands of *Phragmites australis* and *Typha domingensis* that improved plant growth, increased in bacterial count and enhanced textile effluent degradation [64]. These methods are cost effective and efficient to treat textile wastewater. The proposed method in this study is focused on remediation of textile dye contaminated soil which is neglected in the previous studies.

The outcomes of this study revealed that, although bioaugmentation of the microcosms enhanced the degradation of textile effluent in the

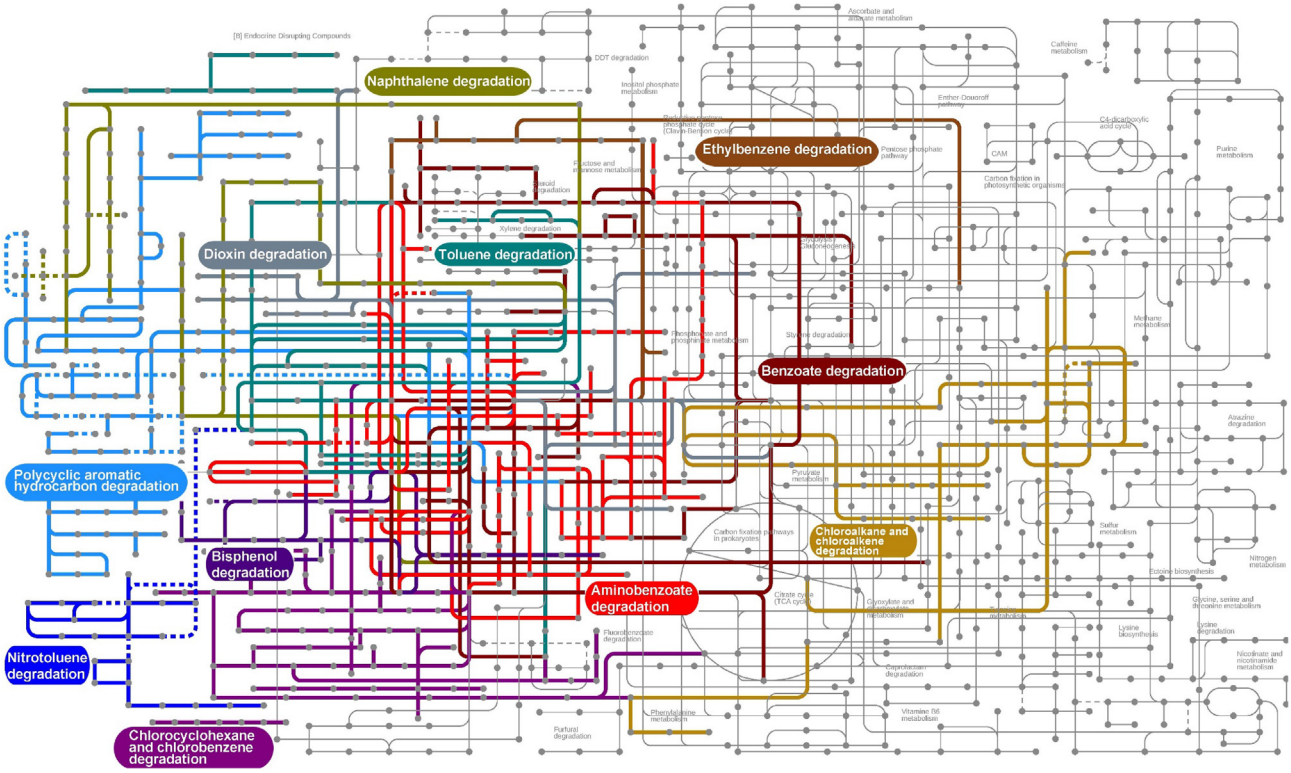

Fig. 8. KEGG map of xenobiotic degradation pathways present in soil microcosms. Pathways highlighted in color were overrepresented (> 50%) due to exposure to textile dye mixture (TDM) and Textile industrial effluent (TIE).

early phase, the indigenous soil microbiome had the capability to recover. However, textile dye exposure had a significant impact on the diversity of the core microbiota in the soil, which may strongly impact on its productivity. The bioaugmentation helped to maintain the indigenous soil microbiota, indicating that bioaugmentation techniques would be beneficial to restore soil productivity. The identified microbial structure contained both aerobic as well as anaerobic degradation pathways, resulting in increased degradation process.

4. Conclusions

The decolorization efficiencies of soil microcosms can be enhanced by augmentation with dye-degrading bacteria at the initial stage by reducing the lag phase. The augmented dye-degrading microbial consortium was able to degrade the dye mixture efficiently and survive. This study provides evidence of a native microbial species have potential bioremediation in contaminated agricultural soils. These core microbiotas can potentially play an important role in the *in-situ* degradation of textile dyes from industrial effluents. The functional annotation illustrated increase in metagene encoding xenobiotic degradation enzymes in microcosm augmented with dye degrading bacteria. The augmentation of dye degrading bacteria can be used as sustainable approach for effective and long-term soil remediation.

Declaration of Competing Interest

The authors declare that they have no known competing financial interests or personal relationships that could have appeared to influence the work reported in this paper.

Acknowledgments

All the authors thankfully acknowledge the financial support from the Korea Environmental Industry Technology Institute (KEITI), the Ministry of Environment (ME) of the Republic of Korea (No. 2018002480007), and the Department of Biotechnology (DBT, New Delhi, India) Interdisciplinary Program of Life Sciences for Advanced Research and Education (BT/PR4572/INF/22/147/2012). We extend our thanks to Dr. Yogesh Shouche, NCMR-NCCS, Pune, for the NGS facilities and some technical support in genomics. SPG is thankful to Hanyang University for the research grants (HY201800000003220).

Authors contributions

The study was planned and performed by SMP, SPG and BHJ. SMP and MVS performed the metagenome sequencing and data analysis. SMP led the interpretation of the results, supported by VVC, MBK, SPG and BHJ. SMP drafted the article, helped by MBK, SPG and BHJ.

Appendix A. Supplementary data

Supplementary data to this article can be found online at https://doi.org/10.1016/j.cej.2019.122533.

References

[1] R.V. Khandare, S.P. Govindwar, Phytoremediation of textile dyes and effluents: current scenario and future prospects, Biotechnol. Adv. 33 (2015) 1697–1714.
[2] Y. Wu, X. Jing, C. Gao, Q. Huang, P. Cai, Recent advances in microbial electrochemical system for soil bioremediation, Chemosphere 211 (2018) 156–163.
[3] O. Gibert, A. Assal, H. Devlin, T. Elliot, R.M. Kalin, Performance of a field-scale biological permeable reactive barrier for *in-situ* remediation of nitrate-contaminated groundwater, Sci. Total Environ. 659 (2019) 211–220.
[4] H. Dongyi, J. Cui, M. Gao, W.Q. Wang, J. Zhou, J. Yang, J. Wang, L. Yong, C. Jiang, Y. Peng, Effects of soil amendments applied on cadmium availability, soil enzyme activity, and plant uptake in contaminated purple soil, Sci. Total Environ. 654 (2019) 1364–1371.
[5] J.Q. Xiong, M.B. Kurade, B.H. Jeon, Biodegradation of levofloxacin by an acclimated freshwater microalga, *Chlorella vulgaris*, Chem. Eng. J. 313 (2017) 1251–1257.
[6] D. Ercolini, High-throughput sequencing and metagenomics: moving forward in the culture-independent analysis of food microbial ecology, Appl. Environ. Microbiol. 79 (2013) 3148–3155.
[7] J.A. Fuhrman, Microbial community structure and its functional implications, Nature 459 (2009) 193–199.
[8] S.K. Hansen, P.B. Rainey, J.A. Haagensen, S. Molin, Evolution of species interactions in a biofilm community, Nature 445 (2007) 533–536.
[9] E.M. Brito, R. Duran, R. Guyoneaud, M. Goni-Urriza, T. Garcia de Oteyza, M.A. Crapez, I. Aleluia, J.C. Wasserman, A case study of *in situ* oil contamination in a mangrove swamp (Rio De Janeiro, Brazil), Mar. Pollut. Bull. 58 (2009) 418–423.
[10] F.D. Andreote, D.J. Jimenez, D. Chaves, A.C.F. Dias, D.M. Luvizotto, F. Dini-Andreote, C.C. Fasanella, M.V. Lopez, S. Baena, R.G. Taketani, I. Soares de Melo, The microbiome of Brazilian mangrove sediments as revealed by metagenomics, PLoS ONE 7 (2012) e38600.
[11] H.F. dos Santos, J.C. Cury, F.L. do Carmo, A.L. dos Santos, J. Tiedje, J.D. van Elsas, A.S. Rosado, R.V. Peixoto, Mangrove bacterial diversity and the impact of oil contamination revealed by pyrosequencing: bacterial proxies for oil pollution, PLoS ONE 6 (2011) e16943.
[12] A. Spagni, S. Casu, S. Grilli, Decolourisation of textile wastewater in a submerged anaerobic membrane bioreactor, Bioresour. Technol. 117 (2012) 180–185.
[13] A.M. Lotito, M. De Sanctis, C. Di Iaconi, G. Bergna, Textile wastewater treatment: aerobic granular sludge vs activated sludge systems, Water Res. 54 (2014) 337–346.
[14] M. Punzi, A. Anbalagan, R.A. Borner, B.M. Svensson, M. Jonstrup, B. Mattiasson, Degradation of a textile azo dye using biological treatment followed by photo-Fenton oxidation: evaluation of toxicity and microbial community structure, Chem. Eng. J. 270 (2015) 290–299.
[15] G. Subrahmanyam, J.P. Shen, Y.R. Liu, G. Archana, J.Z. He, Response of ammonia-oxidizing archaea and bacteria to long-term industrial effluent-polluted soils, Gujarat, Western India, Environ. Monit. Assess. 186 (2014) 4037–4050.
[16] B. Drury, E. Rosi-Marshall, J.J. Kelly, Wastewater treatment effluent reduces the abundance and diversity of benthic bacterial communities in urban and suburban rivers, Appl. Environ. Microbiol. 79 (2013) 1897–1905.
[17] Z. Zhou, X. Liu, K. Sun, C. Lin, J. Maa, M. He, W. Ouyang, Persulfate-based advanced oxidation processes (AOPs) for organic-contaminated soil remediation: a review, Chem. Eng. J. 372 (2019) 836–851.
[18] J. Hofman, J. Bezchlebova, L. Dusek, L. Dolezal, I. Holoubek, P. Andel, A. Ansorgova, S. Maly, Novel approach to monitoring of the soil biological quality, Environ. Int. 28 (2003) 771–778.
[19] K. Gkarmiri, R.D. Finlay, S. Alstrom, E. Thomas, M.A. Cubeta, N. Hogberg, Transcriptomic changes in the plant pathogenic fungus *Rhizoctonia solani* AG-3 in response to the antagonistic bacteria *Serratia proteamaculans* and *Serratia plymuthica*, BMC Genomics 16 (2015) 630.
[20] R. Nazir, J.A. Warmink, H. Boersma, J.D. van Elsas, Mechanisms that promote bacterial fitness in fungal-affected soil microhabitats, FEMS Microbiol. Ecol. 71 (2010) 169–185.
[21] M.J. Wargo, D.A. Hogan, Fungal-bacterial interactions: a mixed bag of mingling microbes, Curr. Opin. Microbiol. 9 (2006) 359–364.
[22] I. Benoit, M.H. van den Esker, A. Patyshakuliyeva, D.J. Mattern, F. Blei, M. Zhou, J. Dijksterhuis, A.A. Brakhage, O.P. Kuipers, R.P. de Vries, A.T. Kovács, *Bacillus subtilis* attachment to *Aspergillus niger* hyphae results in mutually altered metabolism, Environ. Microbiol. 17 (2015) 2099–2113.
[23] H.X. Li, B. Xu, L. Tang, J.H. Zhang, Z.G. Mao, Reductive decolorization of indigo carmine dye with *Bacillus* sp MZS10, Int. Biodeter. Biodegrad. 103 (2015) 30–37.
[24] T.R. Waghmode, M.B. Kurade, S.P. Govindwar, Time dependent degradation of mixture of structurally different azo and non azo dyes by using *Galactomyces geotrichum* MTCC 1360, Int. Biodeter. Biodegrad. 65 (2011) 479–486.
[25] L.R. Bergsten-Torralba, M.M. Nishikawa, D.F. Baptista, D.P. Magalhaes, M. da Silva, Decolorization of different textile dyes by *Penicillium simplicissimum* and toxicity evaluation after fungal treatment, Braz. J. Microbiol. 40 (2009) 808–817.
[26] D.S. Srivastava, J. Kolasa, J. Bengtsson, A. Gonzalez, S.P. Lawler, T.E. Miller, P. Munguia, T. Romanuk, D.C. Schneider, M.K. Trzcinski, Are natural microcosms useful model systems for ecology? Trends Ecol. Evol. 19 (2004) 379–384.
[27] N.J. Fredriksson, M. Hermansson, B.M. Wilen, The choice of PCR primers has great impact on assessments of bacterial community diversity and dynamics in a wastewater treatment plant, PLoS ONE 8 (2013) e76431.
[28] M.N. Kathiravan, R. Karthick, K. Muthukumar, *Ex situ* bioremediation of Cr(VI) contaminated soil by *Bacillus* sp.: batch and continuous studies, Chem. Eng. J. 169 (2011) 107–115.
[29] R.V. Khandare, A.D. Watharkar, A.N. Kabra, M.S. Kachole, S.P. Govindwar, Development of a low-cost, phyto-tunnel system using *Portulaca grandiflora* and its application for the treatment of dye-containing wastewaters, Biotechnol. Lett. 36 (2013) 47–55.
[30] APHA, Standard Method for the Examination of Water and Wastewater, 20th ed., American Public Health Association, Washington, DC, U.S.A., 2005.
[31] W.L. Lindsay, W.A. Norvell, Development of a DTPA soil test for zinc, iron, manganese, and copper, Soil Sci. Soc. Am. J. 42 (1978) 421–428.
[32] J. Snajdr, V. Valaskova, V. Merhautova, J. Herinkova, T. Cajthaml, P. Baldrian, Spatial variability of enzyme activities and microbial biomass in the upper layers of Quercus petraea forest soil, Soil Biol. Biochem. 40 (2008) 2068–2075.
[33] A.K. Bartram, M.D. Lynch, J.C. Stearns, G. Moreno-Hagelsieb, J.D. Neufeld, Generation of multimillion-sequence 16S rRNA gene libraries from complex microbial communities by assembling paired-end illumina reads, Appl. Environ. Microbiol. 77 (2011) 3846–3852.
[34] S. Bhute, P. Pande, S.A. Shetty, R. Shelar, S. Mane, S.V. Kumbhare, A. Gawali,

H. Makhani, M. Navandar, D. Dhotre, H. Lubree, D. Agarwal, R. Patil, S. Ozarkar, S. Ghaskadbi, C. Yajnik, S. Juvekar, G.K. Makharia, Y.S. Shouche, Molecular characterization and meta-analysis of gut microbial communities illustrate enrichment of *Prevotella* and *Megasphaera* in Indian subjects, Front. Microbiol. 7 (2016) 660.

[35] P.D. Schloss, S.L. Westcott, T. Ryabin, J.R. Hall, M. Hartmann, E.B. Hollister, R.A. Lesniewski, B.B. Oakley, D.H. Parks, C.J. Robinson, J.W. Sahl, B. Stres, G.G. Thallinger, D.J. Van Horn, C.F. Weber, Introducing mothur: open-source, platform-independent, community-supported software for describing and comparing microbial communities, Appl. Environ. Microbiol. 75 (2009) 7537–7541.

[36] J.G. Caporaso, J. Kuczynski, J. Stombaugh, K. Bittinger, F.D. Bushman, E.K. Costello, N. Fierer, A.G. Pena, J.K. Goodrich, J.I. Gordon, G.A. Huttley, S.T. Kelley, D. Knights, J.E. Koenig, R.E. Ley, C.A. Lozupone, D. McDonald, B.D. Muegge, M. Pirrung, J. Reeder, J.R. Sevinsky, P.J. Turnbaugh, W.A. Walters, J. Widmann, T. Yatsunenko, J. Zaneveld, R. Knight, QIIME allows analysis of high-throughput community sequencing data, Nat. Methods 7 (2010) 335–336.

[37] S.M. Huse, Y.Z. Ye, Y.J. Zhou, A.A. Fodor, A core human microbiome as viewed through 16S rRNA sequence clusters, PLoS ONE 7 (2012) e34242.

[38] D.H. Parks, R.G. Beiko, Identifying biologically relevant differences between metagenomic communities, Bioinformatics 26 (2010) 715–721.

[39] M.G.I. Langille, J. Zaneveld, J.G. Caporaso, D. McDonald, D. Knights, J.A. Reyes, J.C. Clemente, D.E. Burkepile, R.L. Vega Thurber, R. Knight, R.G. Beiko, C. Huttenhower, Predictive functional profiling of microbial communities using 16S rRNA marker gene sequences, Nat. Biotechnol. 31 (2013) 814–821.

[40] H. Heberle, G.V. Meirelles, F.R. da Silva, G.P. Telles, R. Minghim, InteractiVenn: a web-based tool for the analysis of sets through Venn diagrams, BMC Bioinf. 16 (2015) 169.

[41] L. Ayed, K. Chaieb, A. Cheref, A. Bakhrouf, Biodegradation and decolorization of triphenylmethane dyes by *Staphylococcus epidermidis*, Desalination 260 (2010) 137–146.

[42] R.L. Stingley, W. Zou, T.M. Heinze, H. Chen, C.E. Cerniglia, Metabolism of azo dyes by human skin microbiota, J. Med. Microbiol. 59 (2010) 108–114.

[43] O. Anjaneya, S.Y. Souche, M. Santoshkumar, T.B. Karegoudar, Decolorization of sulfonated azo dye Metanil yellow by newly isolated bacterial strains: *Bacillus* sp. strain AK1 and *Lysinibacillus* sp. strain AK2, J. Hazard. Mater. 190 (2011) 351–358.

[44] A. Guadie, S. Tizazu, M. Melese, W. Guo, H.H. Ngo, S. Xia, Biodecolorization of textile azo dye using *Bacillus* sp. strain CH12 isolated from alkaline lake, Biotechnol. Rep. (Amst) 15 (2017) 92–100.

[45] V.V. Chandanshive, S.K. Kadam, R.V. Khandare, M.B. Kurade, B.H. Jeon, J.P. Jadhav, S.P. Govindwar, In situ phytoremediation of dyes from textile wastewater using garden ornamental plants, effect on soil quality and plant growth, Chemosphere 210 (2018) 968–976.

[46] N. Shen, Y.C. Huo, J.J. Chen, F. Zhang, H. Zheng, R.J. Zeng, Decolorization by *Caldicellulosiruptor saccharolyticus* with dissolved hydrogen under extreme thermophilic conditions, Chem. Eng. J. 262 (2015) 847–853.

[47] F. Shen, Y. Li, M. Zhang, M.K. Awasthi, A. Ali, R. Li, Q. Wang, Z. Zhang, Atmospheric deposition-carried Zn and Cd from a zinc smelter and their effects on soil microflora as revealed by 16S rDNA, Sci. Rep. 6 (2016) 39148.

[48] M.B. Kurade, T.R. Waghmode, S.M. Patil, B.H. Jeon, S.P. Govindwar, Monitoring the gradual biodegradation of dyes in a simulated textile effluent and development of a novel triple layered fixed bed reactor using a bacterium-yeast consortium, Chem. Eng. J. 307 (2017) 1026–1036.

[49] J. Guo, J. Zhou, D. Wang, C. Tian, P. Wang, M.S. Uddin, H. Yu, Biocalalyst effects of immobilized anthraquinone on the anaerobic reduction of azo dyes by the salt-tolerant bacteria, Water Res. 41 (2007) 426–432.

[50] S.S. Phugare, D.C. Kalyani, A.V. Patil, J.P. Jadhav, Textile dye degradation by bacterial consortium and subsequent toxicological analysis of dye and dye metabolites using cytotoxicity, genotoxicity and oxidative stress studies, J. Hazard. Mater. 186 (2011) 713–723.

[51] A. Bafana, T. Chakrabarti, K. Krishnamurthi, S.S. Devi, Biodiversity and dye decolourization ability of an acclimatized textile sludge, Bioresour. Technol. 99 (11) (2008) 5094–5098.

[52] N.B. Sutton, F. Maphosa, J.A. Morillo, W.A. Al-Soud, A.A. Langenhoff, T. Grotenhuis, H.H.M. Rijnaarts, H. Smidt, Impact of long-term diesel contamination on soil microbial community structure, Appl. Environ. Microbiol. 79 (2013) 619–630.

[53] M. Peng, X. Zi, Q. Wang, Bacterial community diversity of oil-contaminated soils assessed by high throughput sequencing of 16S rRNA genes, Int. J. Environ. Res. Public Health 12 (2015) 12002–12015.

[54] F. Abbasian, T. Palanisami, M. Megharaj, R. Naidu, R. Lockington, K. Ramadass, Microbial diversity and hydrocarbon degrading gene capacity of a crude oil field soil as determined by metagenomics analysis, Biotechnol. Prog. 32 (2016) 638–648.

[55] C. Averill, B.L. Turner, A.C. Finzi, Mycorrhiza-mediated competition between plants and decomposers drives soil carbon storage, Nature 505 (2014) 543–545.

[56] M.G. van der Heijden, F.M. Martin, M.A. Selosse, I.R. Sanders, Mycorrhizal ecology and evolution: the past, the present, and the future, New Phytol. 205 (2015) 1406–1423.

[57] D.K. Sharma, H.S. Saini, M. Singh, S.S. Chimni, B.S. Chadha, Isolation and characterization of microorganisms capable of decolorizing various triphenylmethane dyes, J. Basic Microbiol. 44 (1) (2004) 59–65.

[58] B.D. Tony, D. Goyal, S. Khanna, Decolorization of textile azo dyes by aerobic bacterial consortium, Int. Biodeter. Biodegrad. 63 (2009) 462–469.

[59] N. Ali, A. Hameed, S. Ahmed, Physicochemical characterization and bioremediation perspective of textile effluent, dyes and metals by indigenous bacteria, J. Hazard. Mater. 164 (2010) 322–328.

[60] S.K. Kadam, V.V. Chandanshive, N.R. Rane, S.M. Patil, A.R. Gholave, R.V. Khandare, A.R. Bhosale, B.H. Jeon, S.P. Govindwar, Phytobeds with *Fimbristylis dichotoma* and *Ammannia baccifera* for treatment of real textile effluent: an *in-situ* treatment, anatomical studies and toxicity evaluation, Environ. Res. 160 (2018) 1–11.

[61] X.Y. Cheng, X.L. Tian, Y.S. Wang, R.M. Lin, Z.C. Mao, N. Chen, B.Y. Xie, Metagenomic analysis of the pinewood nematode microbiome reveals a symbiotic relationship critical for xenobiotics degradation, Sci. Rep. 3 (2013) 1869.

[62] G.D. Gikas, M. Pérez-Villanueva, M. Tsioras, C. Alexoudis, G. Pérez-Rojas, M. Masís-Mora, V. Lizano-Fallas, C.E. Rodríguez-Rodríguez, Z. Vryzas, V.A. Tsihrintzis, Low-cost approaches for the removal of terbuthylazine from agricultural wastewater: constructed wetlands and biopurification system, Chem. Eng. J. 335 (2018) 647–656.

[63] S.K. Mallick, S. Chakraborty, Bioremediation of wastewater from automobile service station in anoxic-aerobic sequential reactors and microbial analysis, Chem. Eng. J. 361 (2019) 982–989.

[64] N. Tara, M. Iqbal, Q.M. Khan, M. Afzal, Bioaugmentation of floating treatment wetlands for the remediation of textile effluent, Water Environ. J. 33 (2019) 124–134.